COMPDYN 2013
4th ECCOMAS Thematic Conference on
Computational Methods in Structural Dynamics and Earthquake Engineering
M. Papadrakakis, V. Papadopoulos, V. Plevris (eds.)
Kos Island, Greece, 12–14 June 2013

SEISMIC SOIL-PILE INTERACTION — INFLUENCE OF SOIL INELASTICITY

Andreas E. Kampitsis[1], Evangelos J. Sapountzakis[2], Spyros K. Giannakos[3] and Nikos A. Gerolymos[4]

[1] School of Civil Engineering, National Technical University of Athens
Zografou Campus, GR-157 80, Athens, Greece

e-mail: cvakamb@gmail.com [2] e-mail: cvsapoun@central.ntua.gr
[3] e-mail: spigian@hotmail.com [4] e-mail: gerolymos@gmail.com

Keywords: Soil–Pile–Structure Interaction, Nonlinear Winkler, Nonlinear Dynamics, Large Deflections, BEM– FEM.

Abstract. *The main purpose of this study is to investigate the influence of soil p-y nonlinearity in soil–pile–structure kinematic and inertia interaction. Within this context, a beam on nonlinear Winkler foundation model is adopted based on the Boundary Element Method (BEM), accounting for the effects induced by geometrical nonlinearity, rotary inertia and shear deformation, employing the concept of shear deformation coefficients. The soil nonlinearity is taken into consideration by means of a hybrid spring configuration consisting of a nonlinear (*p-y*) spring connected in series to an elastic spring–damper model. The nonlinear spring captures the near–field plastification of the soil while the spring–damper system represents the far–field viscoelastic character of the soil. An extensive case study is carried out on a pile–column–deck system of a bridge, founded in two cohesive layers of sharply different stiffness and subjected in various earthquake excitations.*

1 INTRODUCTION

The seismic response of column-pile systems under transient earthquake excitation is an area of extensive active research, since pile foundation is widely used to support superstructures such as bridges, wind-turbines and offshore platforms. As the seismic shear wave propagates through the soil deposit, the embedded foundation tends to modify the transmitted excitation due to the soil–foundation stiffness contrast, the boundary constrains of the head and tip of the pile as well as the dynamic response of the system (frequency correlation). This interaction develops even in the absence of a superstructure and is referred to as the *kinematic interaction*. At the same time, the dynamic response of the superstructure itself induces additional deformations to the pile and the near–field soil. This effect is known as *inertial interaction. Kinematic and inertial interaction* constitute a complex and unique phenomenon referred to as *Soil–Pile–Structure Interaction* (SPSI) which includes a number of parameters, such as the soil stratigraphy and properties, the non–linear stress–strain behavior of the soil and pile (material nonlinearity) and the geometrical nonlinearities (p–δ effects, separation and slippage).

The main purpose of this study is to investigate the influence of soil p-y nonlinearity in soil–pile–structure kinematic and inertia interaction. Within this context, a beam on nonlinear Winkler foundation model is adopted based on the Boundary Element Method (BEM), accounting for the effects induced by geometrical nonlinearity, rotary inertia and shear deformation, employing the concept of shear deformation coefficients. The soil nonlinearity is taken into consideration by means of a hybrid spring configuration consisting of a nonlinear (p-y) spring connected in series to an elastic spring–damper model. The nonlinear spring captures the near–field plastification of the soil while the spring–damper system (Kelvin–Voigt element) represents the far–field viscoelastic character of the soil. An extensive case study is carried out on a pile–column–deck system of a bridge, founded in two cohesive layers of sharply different stiffness and subjected in various earthquake excitations, providing insight to several phenomena. The results of the proposed model are compared with those obtained from the Beam–FE model employing OpenSees code [1] as well as from a rigorous fully three-dimensional (3–D) continuum FE scheme materialized in the ABAQUS code [2]. The essential features and novel aspects of the present contribution compared with previous ones are summarized as follows.

i. Soil nonlinearity is taken under consideration by means of a hybrid spring configuration consisting of a nonlinear (p-y) spring for the near–field plastification, connected in series to a Kelvin–Voigt element representing the far–field viscoelastic character of the soil.
ii. A calibration methodology of the "spring" and "dashpot" coefficients of the examined hybrid spring configuration is proposed.
iii. Verification of the computational efficiency of the proposed model through the remarkable agreement between its results and those from the sophisticated 3–D model. Moreover, the increased accuracy of the proposed procedure compared with other FEM solutions employing also beam elements is demonstrated.
iv. The proposed method is capable of taking into account both kinematic and inertia interaction to the geometrical nonlinear dynamic response of a column-pile in a layered soil profile.
v. The site seismic response is obtained through one dimensional shear wave propagation analysis.
vi. The pile head and tip are supported by the most general nonlinear boundary conditions. Although a circular pile cross section is investigated, the formulation is capable of analyzing an arbitrary doubly symmetric one.

vii. Shear deformation effect and rotary inertia are taken into account on seismic pile–soil–structure interaction.

2 PROPOSED BEAM FORMULATION

Let us consider a cylindrical column-pile of length l (pile length L, pier length H), diameter d, mass density ρ_p, modulus of elasticity E_p, shear modulus G_p and Poisson's ratio v_p, as this is presented in Fig.1. The pile is embedded in a layered soil profile of Winkler type, materialized by a hybrid spring configuration. As proposed by Wang et al. [3], the soil is separated into two zones, namely a near–field zone implemented by Kelvin–Voigt element (k_{el}, c_{el}) and a far–field one represented by hysteretic element (k_{nl}). More specifically, the adopted hybrid model consists of a nonlinear spring connected in series to a dashpot–elastic spring parallel configuration. The free extremities of the configuration are excited by the free–field (w_{ff}, $\dot{w}_{ff}$) displacement and velocities time histories obtained at each depth from the free–field seismic response analysis (Fig.1).

The column-pile is subjected to the combined action of arbitrarily distributed or concentrated time dependent transverse loading $p_z = p_z(x,t)$ as well as to axial loading $p_x = p_x(x,t)$. Under these actions, the displacement field taking into account shear deformation effect is given as [4]

$$\overline{u}(x,z,t) = u(x,t) + z\theta_y(x,t) \tag{1a}$$

$$\overline{w}(x,t) = w(x,t) \tag{1b}$$

where $\overline{u}$, $\overline{w}$ are the axial and transverse displacement components with respect to the Cyz centroidal coordinate system of axes (Fig.1); $u(x,t)$, $w(x,t)$ are the corresponding components of the centroid C and $\theta_y(x,t)$ is the angle of rotation due to bending of the cross-section with respect to its centroid. It is worth here noting that since the additional angle of rotation of the cross-section due to shear deformation is taken into account, the one due to bending is not equal to the derivative of the deflection (i.e. $\theta_y \neq w'$).

Adopting the strain-displacement relations of the three-dimensional elasticity for moderate displacements and small strains, employing the second Piola–Kirchhoff stress tensor, the governing differential equations and the boundary conditions of the examined problem are obtained based on Hamilton's principle [4]. Following this procedure, the governing equations for the problem at hand are written as

$$\rho_p \mathrm{A}\ddot{u} - E_p A\left(u'' + w'w''\right) = p_x \tag{2a}$$

$$\rho_p \mathrm{A}\ddot{w} - \left(Nw'\right)' - G_p A_z\left(w'' + \theta_y'\right) + k_{nl}\left(w - w_{mnode}\right) = p_z \tag{2b}$$

$$E_p I_y \theta_y'' - G_p A_z\left(w' + \theta_y\right) = \rho_p I_y \ddot{\theta}_y \tag{2c}$$

while the equilibrium of forces at the mid-node of the spring configuration results in an additional equation

$$k_{el}\left(w_{mnode} - w_{ff}\right) + c_{el}\left(\dot{w}_{mnode} - \dot{w}_{ff}\right) = k_{nl}\left(w - w_{mnode}\right) \tag{3}$$

where, $w_{ff} = w_{ff}(z,t)$, $\dot{w}_{ff} = \dot{w}_{ff}(z,t)$ and w_{mnode}, $\dot{w}_{mnode}$ correspond to the free-field and mid-node displacement and velocity, respectively. Moreover, the corresponding time dependent boundary conditions of the problem at hand are given as

$$a_1 u(x,t) + \alpha_2 N(x,t) = \alpha_3 \tag{4}$$

$$\beta_1 w(x,t) + \beta_2 V_z(x,t) = \beta_3 \qquad \gamma_1 \theta_y(x,t) + \gamma_2 \mathrm{M}_y(x,t) = \gamma_3 \tag{5,6}$$

at the column-pile ends $x = 0, l$, together with the initial conditions

$$u(x,0) = \overline{u}_0(x) \qquad \dot{u}(x,0) = \dot{\overline{u}}_0(x) \tag{7a,b}$$

$$w(x,0) = \overline{w}_0(x) \qquad \dot{w}(x,0) = \dot{\overline{w}}_0(x) \tag{8a,b}$$

$$\theta_y(x,0) = \overline{\theta}_{y0}(x) \qquad \dot{\theta}_y(x,0) = \dot{\overline{\theta}}_{y0}(x) \tag{9a,b}$$

In eqns. (2), A is the cross section area, I_y is the moment of inertia with respect to z-axis and GA_z is its shear rigidity of the Timoshenko's beam theory where $A_z = \kappa_z A = (1/a_z) A$ is the shear area, κ_z the shear correction factor and a_z the shear deformation coefficient. This coefficient is evaluated using an energy approach [5]. Moreover, in eqns. (7)–(9), $\overline{u}_0(x)$, $\overline{w}_0(x)$, $\dot{\overline{u}}_0(x)$, $\dot{\overline{w}}_0(x)$, $\overline{\theta}_{y0}$ and $\dot{\overline{\theta}}_{y0}$ are prescribed functions, while in eqns. (4)–(6), N is the axial force, V_z is the transversal force and M_y is the bending moment at the ends of the column-pile accounting for the inertia forces induced from the mass of the superstructure. Finally, α_k, β_k, γ_k ($k = 1, 2, 3$) are functions specified at the column-pile ends $x = 0, l$. Eqns. (4)-(6) describe the most general nonlinear boundary conditions associated with the problem at hand and can include elastic support or restraint. It is apparent that all types of the conventional boundary conditions (clamped, simply supported, free or guided edge) can be derived from these equations by specifying appropriately these functions (e.g. for a free edge it is $\alpha_2 = \beta_2 = \gamma_2 = 1$, $\alpha_1 = \alpha_3 = \beta_1 = \beta_3 = \gamma_1 = \gamma_3 = 0$).

Moreover, a calibration methodology of the "spring" and "dashpot" coefficients of the examined hybrid spring configuration is proposed. The lateral soil reaction against a deflecting pile is expressed as the sum of a hysteretic elastic–perfectly plastic and a visco–plastic component, according to the lumped parameter model, as depicted in Fig. 1. In this way, the frequency–dependent characteristics of the subgrade reaction are realistically captured through a series–parallel assembly of frequency–independent springs and dashpots. In the elastic regime and assuming a sufficiently under-damped response, the small–amplitude frequency–dependent "spring" and "dashpot" coefficients for the lateral soil reaction are approximated by:

$$k_x \approx \frac{k_{el}}{1 + \dfrac{k_{el}}{k_{nl}} + \dfrac{\omega c_{el}}{k_{nl}}} \quad \text{and} \quad c_x \approx \frac{c_{el}}{1 + \dfrac{k_{el}}{k_{nl}} + \dfrac{\omega c_{el}}{k_{nl}}} \tag{10,11}$$

in which ω is the circular frequency. The parameters k_{el}, c_{el} and k_{nl} are appropriately calibrated through an optimization procedure to match the stiffness and dashpot coefficients (Fig. 2) proposed by Makris and Gazetas [6]:

$$k_x = 1.2E_s \quad \text{and} \quad c_x = 6a_0^{-1/4}\rho_s V_s d \tag{12,13}$$

in which E_s, V_s and ρ_s are the Young's modulus, shear wave velocity and mass density of the supporting soil, and α_0 is a dimensionless frequency parameter defined as:

$$\alpha_0 = \frac{\omega d}{V_s} \tag{14}$$

Having calibrated the stiffness k_x and dashpot coefficient c_x according to Eqns. (12) and (13), plastic behavior is then introduced by imposing a threshold value for the reaction force of spring k_{nl} equal to the ultimate soil resistance per unit length of the pile (p_{ult}) as determined by Matlock [7] and Reese et al [8] at near surface (top layer) and at greater depths (bottom layer), respectively. Obviously, when p_{ult} is reached the arranged in-parallel spring and dashpot unit is deactivated and the radiation damping vanishes.

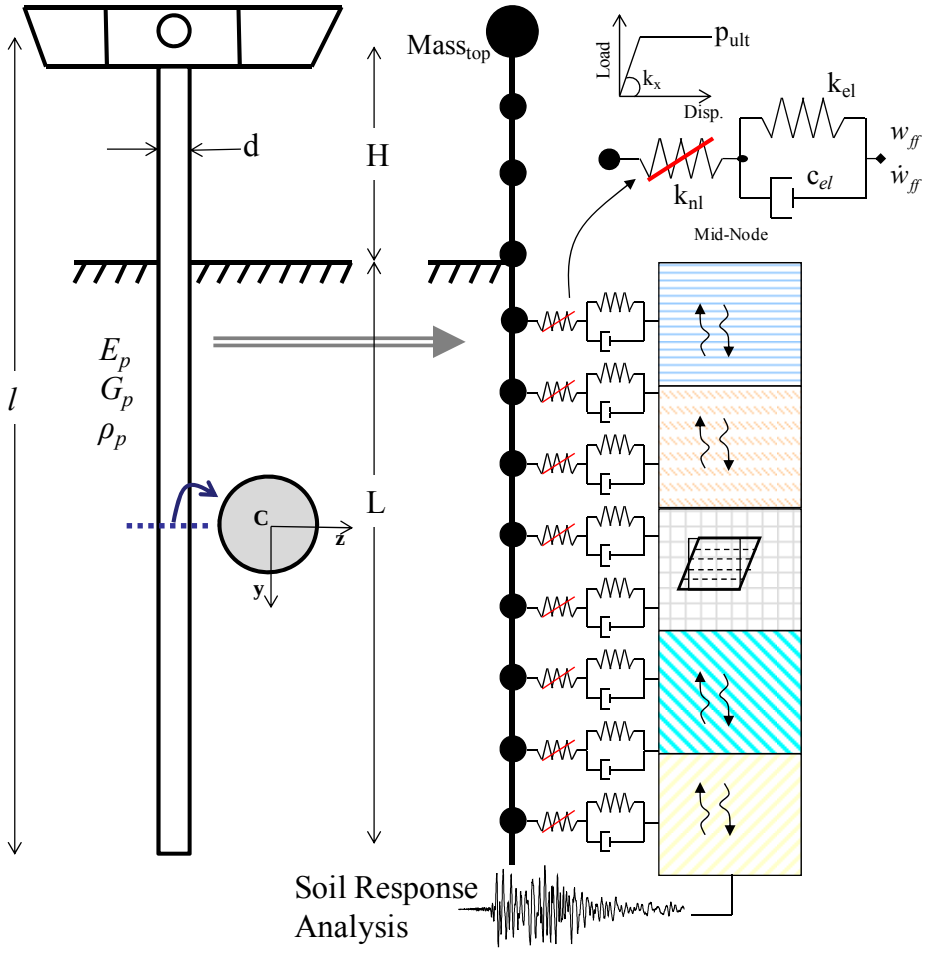

Figure 1: Soil–pile–structure system and adopted model

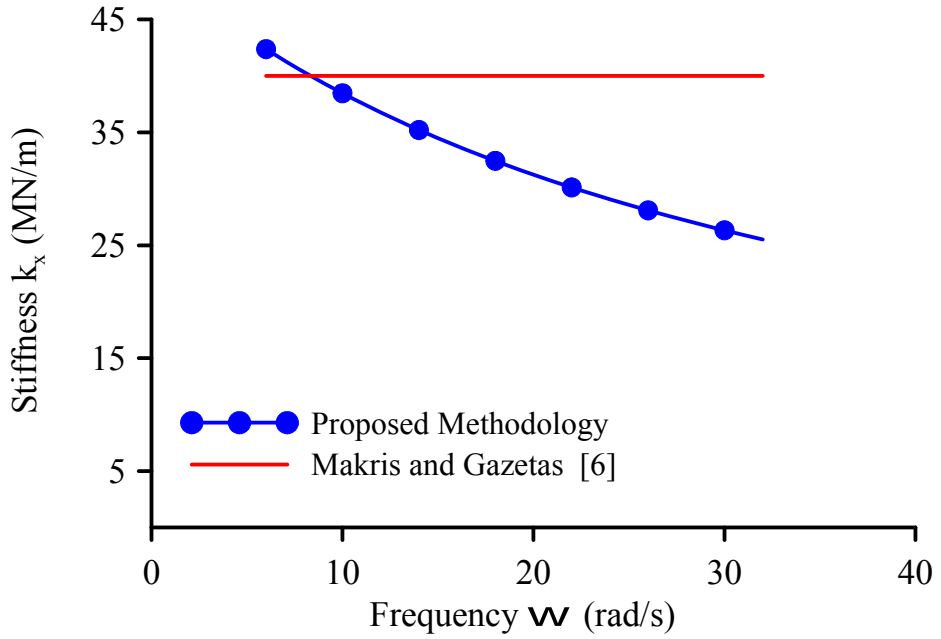

(a)

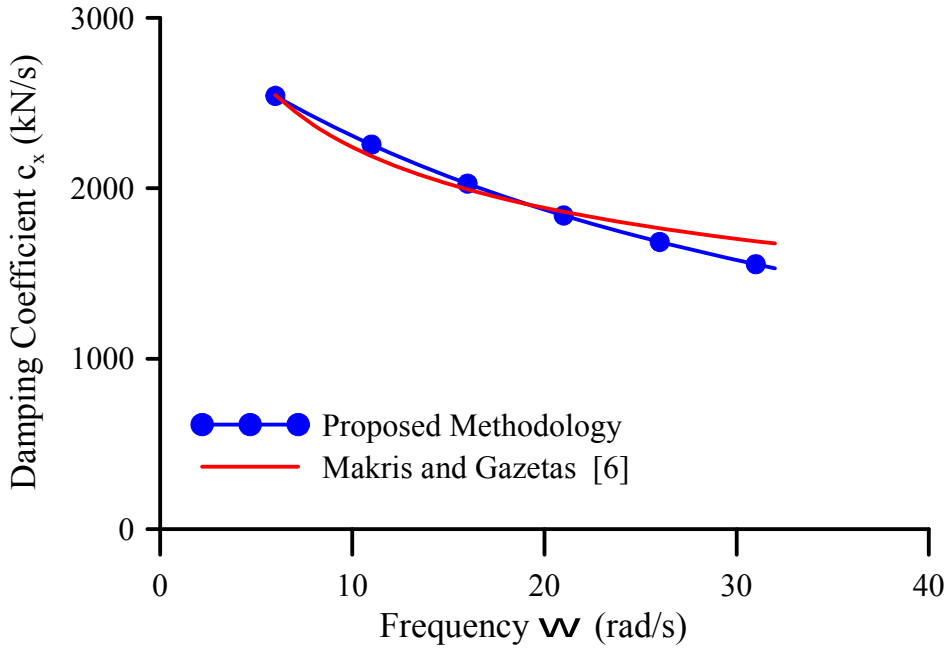

(b)

Figure 2: Calibration of stiffness k_x (a) and damping coefficient c_x (b) for the examined configuration.

3 NUMERICAL SOLUTION

According to the precedent analysis, the geometrically nonlinear soil-pile-structure kinematic and inertia seismic interaction of Timoshenko column-pile embedded in a layered nonlinear Winkler-type soil profile, undergoing moderate large deflections reduces in establishing the displacement components $u(x,t)$, $w(x,t)$ and $\theta_y(x,t)$ having continuous derivatives up to the second order with respect to both space x and time t variables. These displacement components must satisfy the coupled governing differential equations (2), (3) inside the column-pile, the boundary conditions (4)-(6) at the pile ends $x = 0,\ l$ and the initial conditions (7)-(9). Application of the boundary element technique yields a system of nonlinear coupled differential-algebraic equations (DAE) of motion, which can be solved iteratively using any efficient direct time integration scheme. In this study, the Petzold-Gear method is used [9] after introducing new variables to reduce the order of the system [10] and obtain an equivalent system with a value of system index $\text{ind} = 1$ [10].

4 MODEL VERIFICATION AND INTERPRETATION OF RESULTS

4.1 Case study

A column-pile monolithically connected to the bridge deck is embedded in two layers of cohesive soil and excited by seismic motion. The concentrated mass at the centre of the deck is $M_{top} = 60tons$, the height of the pier is $H = 10m$, the embedment length of the pile is $L = 30m$, and the diameter of the column-pile equals to $d = 1.5m$. The column-pile is assumed to be linear elastic, while the idealized soil profile from the Agios Stefanos bay was used for the ground response analyses. A soft to medium normally consolidated clay sets on top of a stiff clay. The bedrock is assumed at $50m$ depth. The soft clay has a thickness of $18m$ and a plasticity index $\text{PI}(\%) = 35$. The second layer is 32m thick and has constant undrained shear strength of 100kPa. The maximum shear modulus was calculated by the empirical equations of Seed and Idriss [11].

The influence of shaking on the seismic response is investigated by selecting three well known acceleration records as seismic excitations:

i) the record from Aegion earthquake (1995)
ii) the record from Lefkada earthquake (2003)
iii) the JMA record from Kobe earthquake (1995)

The first two records were chosen as two strong motions of the seismic environment of Greece, with one and many cycles, respectively. JMA record is used to investigate the dynamic response of the soil-pile-structure system to a quite unfavorable incident. All the records were first scaled to a Peak Grand Acceleration (PGA) of $0.5g$ and $0.8g$ at the ground surface. Then, through deconvolution analyses conducted with SHAKE91 [12], the bedrock motion as well as the motion at various depths along the pile were estimated.

Both elastic and inelastic soil response are investigated. For the elastic soil response, the proposed beam model is verified against a Beam–FE solution and a refined 3–D continuum FE approach. For the inelastic soil response, the proposed model is verified only against the Beam–FE solution due to the fact that soil response in the 3–D continuum FEM strongly depends on the adopted soil constitutive model

4.2 Additional numerical models

The response of the soil–pile–structure system is investigated further with two different methods; namely a simplified Beam–FE model employing the OpenSees code [1], and a rigorous fully 3–D continuum FE scheme materialized in the ABAQUS [2] code.

In the first model a beam supported in discrete springs is used to model the lateral static and dynamic response of a pile. For seismic loadings, free–field soil response is calculated separately from site response analysis [12] and the obtained displacement time histories are applied to the ends of the soil springs.

In the fully 3–D model the calculations of the site response and the soil–pile–structure interaction are performed in a fully coupled manner with the Finite Element Code ABAQUS [2]. The pile–column and the soil behavior are assumed to be elastic, while P-δ effects (linearized 2nd order analysis) are also taken into account. The soil is modeled with 8-node brick elements. The free-field boundaries were investigated by two different types of boundaries; namely 3 dashpots on each node on the boundaries and alternatively appropriate kinematic constraints i.e. Multi-Point Constrains (MPC) boundaries. The comparison of the acceleration, displacement and rotation time histories at the deck level of the 3–D FE model with the both the boundary types provide identical results. Hence, the MPC boundaries were selected for all of the analyses conducted.

4.3 Results and comparison

The numerical results have been obtained using a set of 6 excitation motions. More specifically, in Figs 3–5 the acceleration time histories at the bridge deck level $\ddot{w}(H,t)$ corresponding to the Lefkada, JMA and Aegion excitation motions scaled to $a_g = 0.8g$, are presented, respectively. In these figures the geometrically linear and nonlinear analysis of the proposed model, taking into account both rotary inertia and shear deformation effect are compared with the Beam-FE and the fully 3–D FE models. From the obtained results it is observed that the proposed nonlinear formulation can capture accurately the response of the 3–D FE model accounting for P–δ effect, while the linear case predicts identical acceleration time histories with the Beam–FE model. From the conducted investigation, it is deduced that instead of executing time–expensive 3–D analyses for the soil–pile–bridge system, the proposed beam model can be employed providing minimum calculation effort while retaining high precision in the obtained results.

Moreover, Figs 6–9 illustrate the displacement time histories at the deck level $w(H,t)$ corresponding to the Lefkada, JMA and Aegion excitation motions, respectively taking into account or ignoring *p-y* soil nonlinearity. Finally, in Tables 1, 2 and 3 the extreme values of the bending moment along with their location are presented for different cases of analysis for all the excitation motions. Both the results from the elastic and the inelastic soil response are illustrated. From these figures and tables it is concluded that the proposed geometrically nonlinear formulation captures accurately the calculated response according to the other methods of analysis used, while all the models predict similar shapes of the moment distribution and the increase of the bending moment at the interface of the two soil layers. The models also predict the same depth of the maximum bending moment as well as the shift of the maximum bending moment at a higher depth as the peak ground acceleration increases for the case of the inelastic soil response.

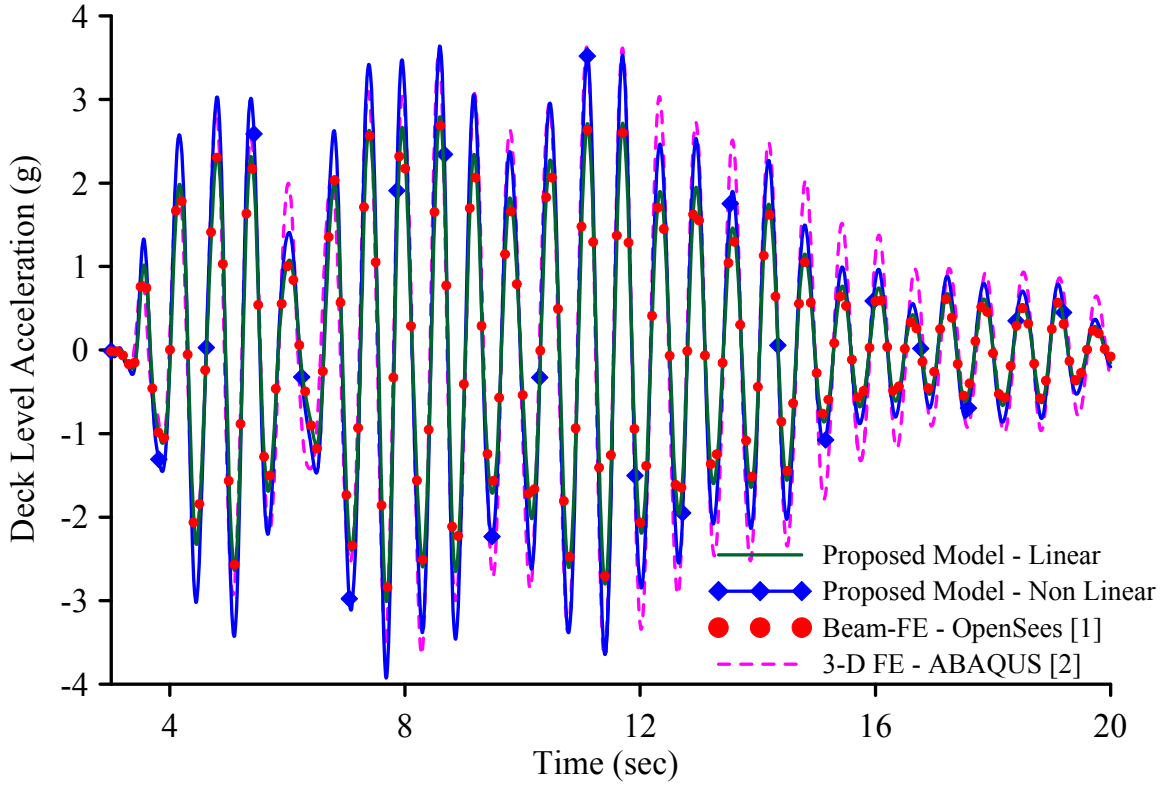

Figure 3: Acceleration time history of the deck level for Lefkada excitation ($a_g = 0.8$g).

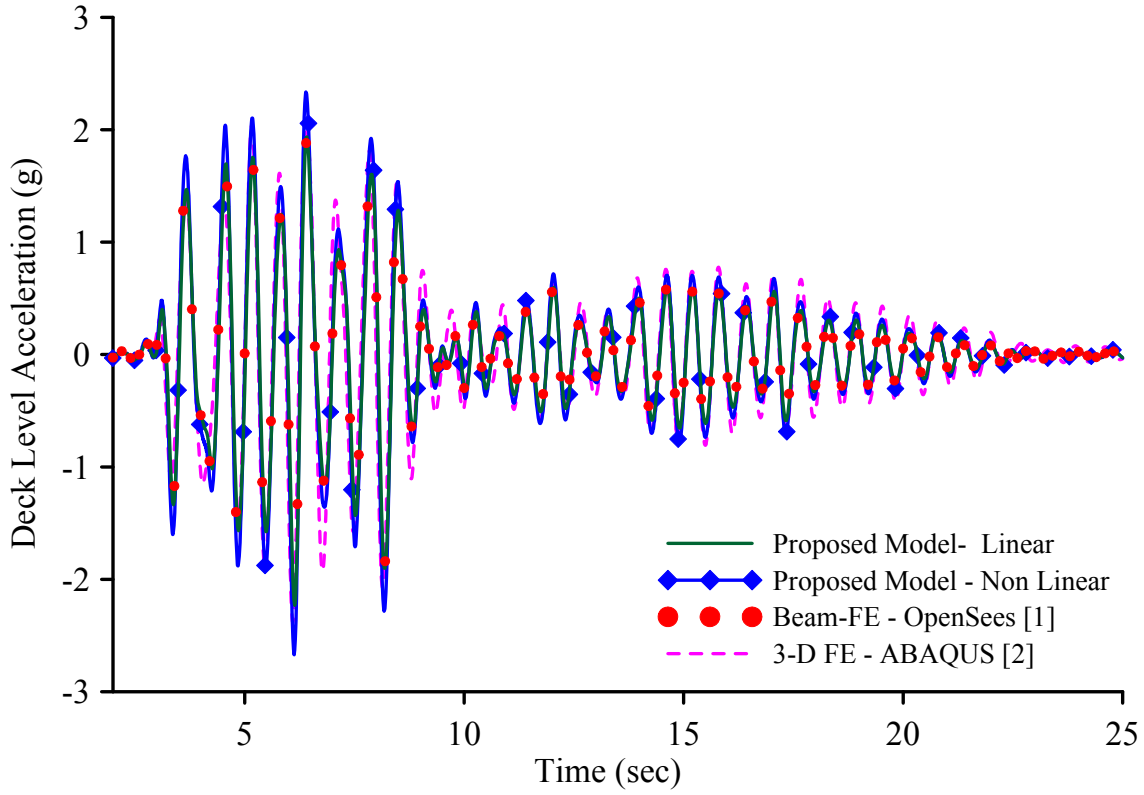

Figure 4: Acceleration time history of the deck level for JMA excitation ($a_g = 0.8g$).

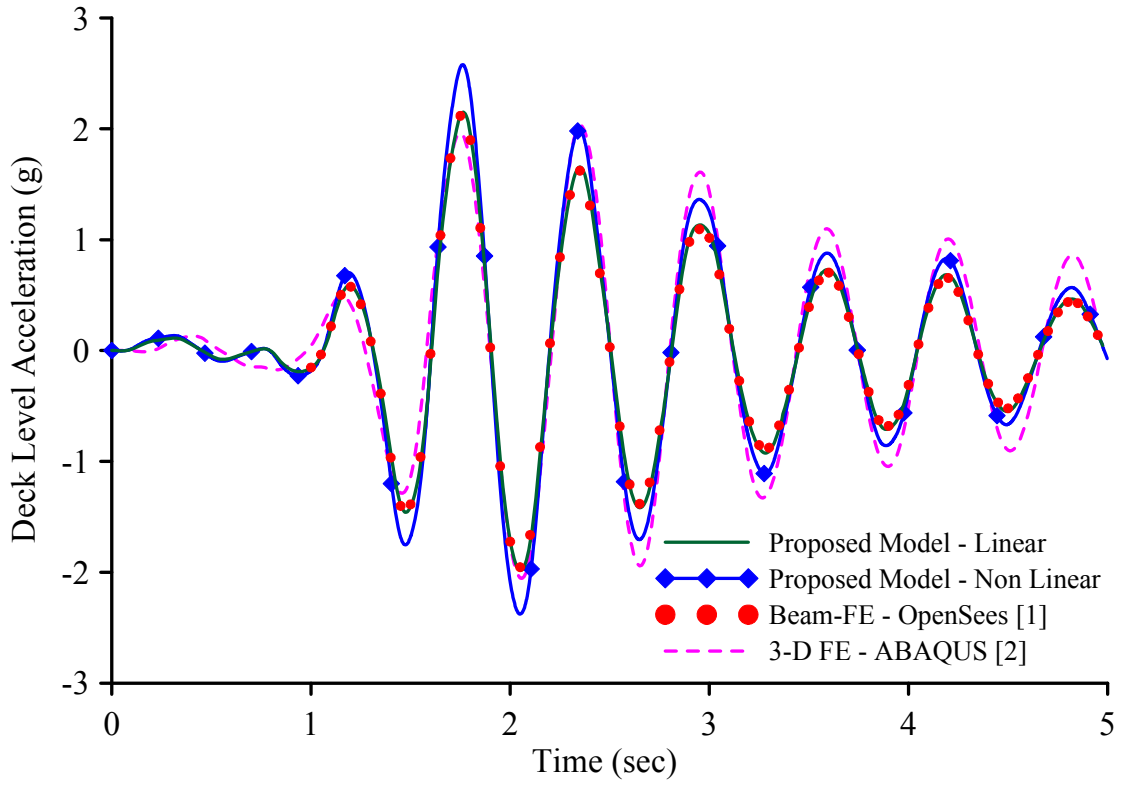

Figure 5: Acceleration time history of the deck level for Aegion excitation ($a_g = 0.8g$).

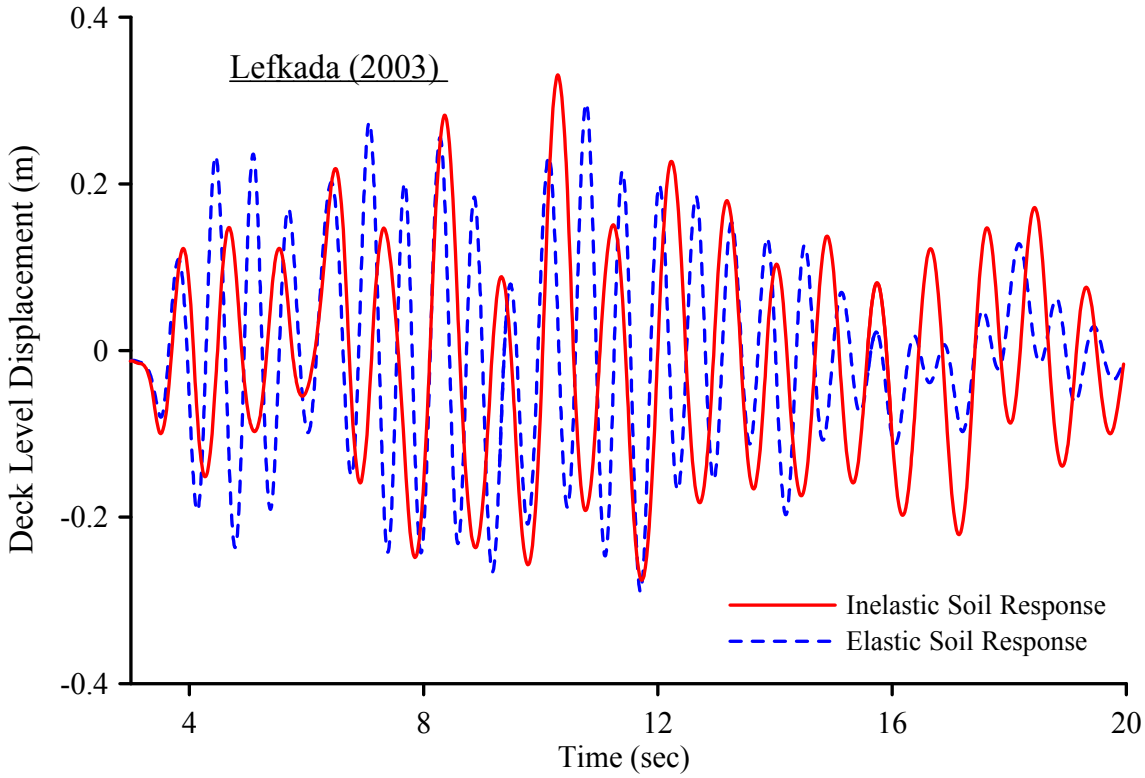

Figure 6: Displacement time history of the deck level for Lefkada excitation ($a_g = 0.8g$).

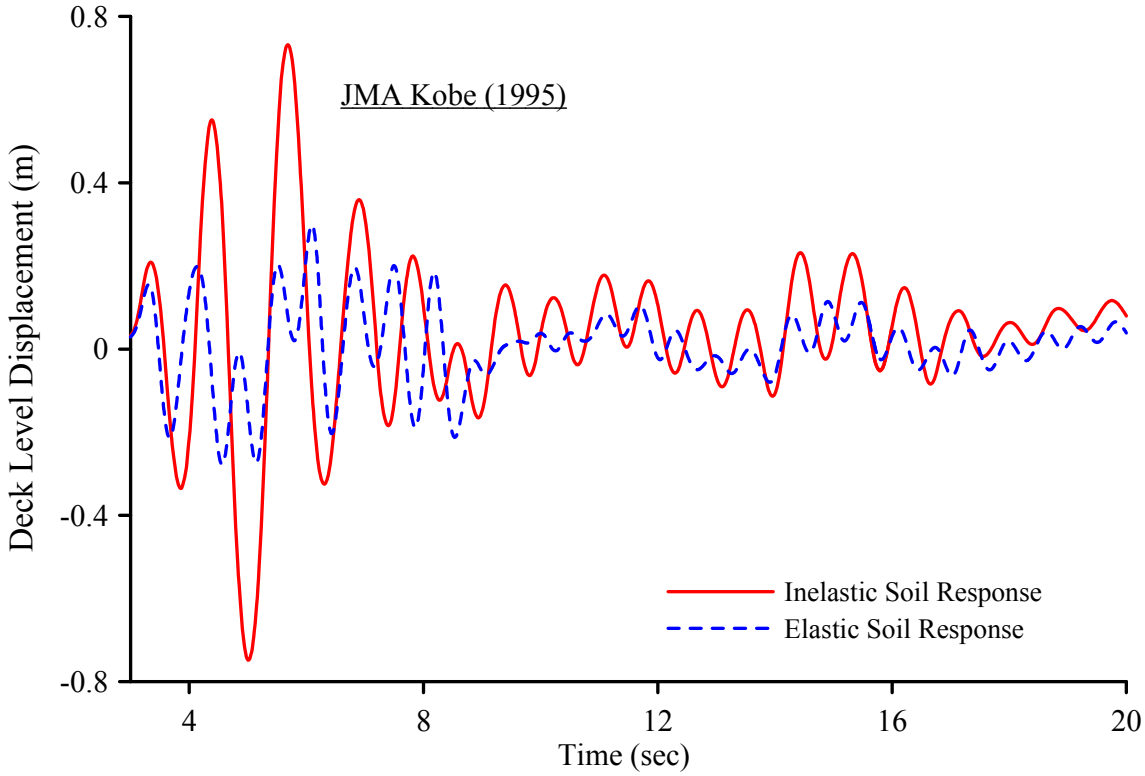

Figure 7: Displacement time history of the deck level for JMA excitation ($a_g = 0.8g$).

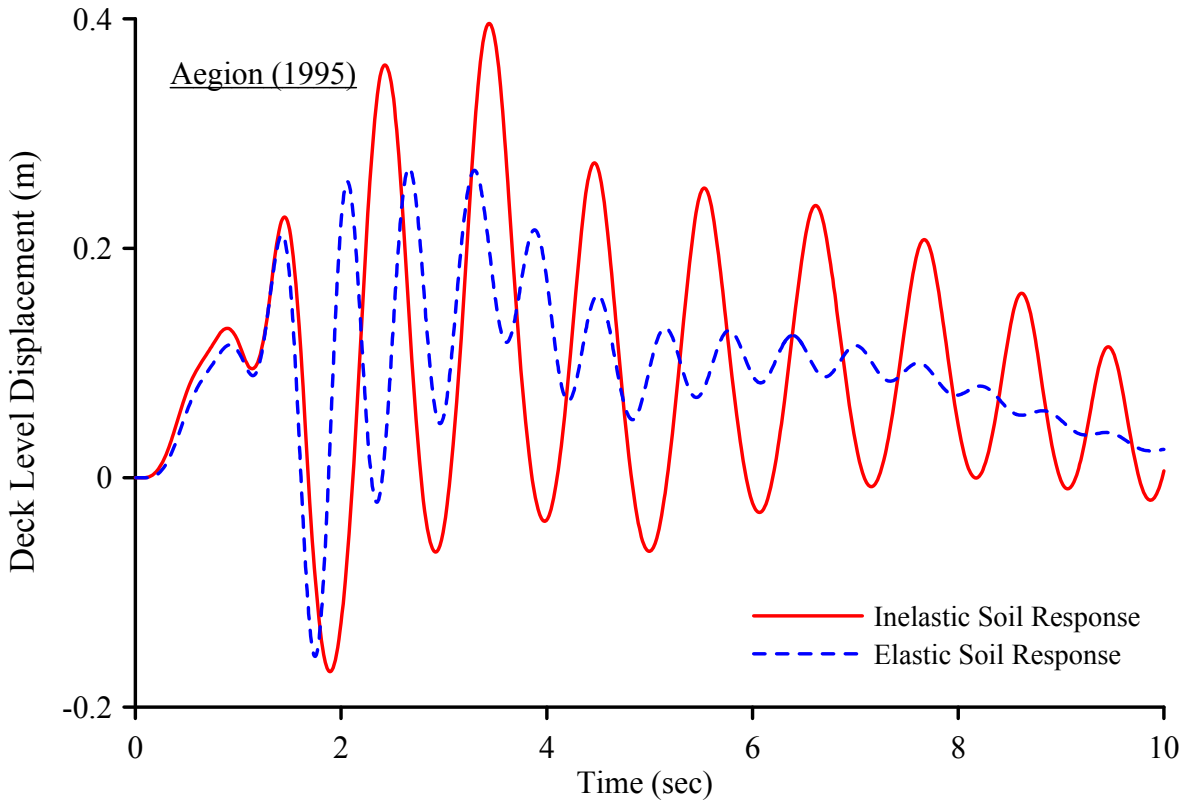

Figure 8: Displacement time history of the deck level for Aegion excitation ($a_g = 0.8g$).

Excitation	Analysis/Model	Elastic Soil		Inelastic Soil	
		M_{el}	Location	M_{pl}	Location
Lefkada (2003) $a_g = 0.5g$	Proposed–Linear	13.68	-1.0	7.19	-4.5
	Proposed–NonLinear	17.01	-1.0	7.16	-4.5
	Beam FE–OpenSees [1]	13.58	-1.0	7.18	-4.5
	3–D FE Abaqus [2]	17.80	-0.5	–	–
Lefkada (2003) $a_g = 0.8g$	Proposed–Linear	21.87	-1.0	12.75	-5.5
	Proposed–NonLinear	27.66	-1.0	12.52	-5.5
	Beam FE–OpenSees [1]	21.72	-1.0	12.60	-5.5
	3–D FE Abaqus [2]	28.48	-0.5	–	–

Table 1: Maximum values of the bending moment for elastic soil M_{el} and inelastic soil M_{pl} in MPa and their location (m) from the ground level, for the Lefkada (2003) excitation motion.

Excitation	Analysis/Model	Elastic Soil		Inelastic Soil	
		M_{el}	Location	M_{pl}	Location
JMA (1995) $a_g = 0.5g$	Proposed–Linear	10.27	-1.0	12.58	-6.5
	Proposed–NonLinear	11.02	-1.0	12.70	-6.5
	Beam FE–OpenSees [1]	10.13	-1.0	12.55	-6.5
	3–D FE Abaqus [2]	11.67	-0.5	.–	–
JMA (1995) $a_g = 0.8g$	Proposed–Linear	16.31	-1.0	19.18	-7.5
	Proposed–NonLinear	17.14	-1.0	19.20	-7.5
	Beam FE–OpenSees [1]	16.21	-1.0	19.16	-7.5
	3–D FE Abaqus [2]	18.67	-0.5	–	–

Table 2: Maximum values of the bending moment for elastic soil M_{el} and inelastic soil M_{pl} in MPa and their location (m) from the ground level, for the Kobe JMA (1995) excitation motion.

5 CONCLUSIONS

In this study, the accuracy of an advanced beam model for the soil–pile–structure kinematic and inertia interaction is investigated and the influence of soil *p-y* nonlinearity is verified. The main conclusions that can be drawn from this investigation are:

- The proposed model takes into account both kinematic and inertia interaction to the geometrical nonlinear dynamic response of a column-pile embedded in a layered soil profile.
- The soil *p-y* nonlinearity strongly influences the system response.
- The proposed formulation captures accurately the response of the 3–D solid model accounting for P-δ effects.
- The proposed model obtains accurate results with minimum computational time required, providing a simple and efficient tool in comparison to fully three dimensional analysis.
- A calibration methodology of the "spring" and "dashpot" coefficients of the examined hybrid spring configuration is proposed.
- The discrepancy between the results of the geometrically linear and the nonlinear analyses is significant especially in the case of an elastic soil behavior.

Excitation	Analysis/Model	Elastic Soil		Inelastic Soil	
		M_{el}	Location	M_{pl}	Location
Aegion (1995) $a_g = 0.5g$	Proposed–Linear	9.94	-1.0	6.75	-4.5
	Proposed–NonLinear	10.00	-1.0	6.72	-4.5
	Beam FE–OpenSees [1]	9.93	-1.0	6.74	-4.5
	3–D FE Abaqus [2]	10.11	-0.5	–	–
Aegion (1995) $a_g = 0.8g$	Proposed–Linear	14.40	-1.0	10.26	-5.5
	Proposed–NonLinear	15.86	-1.0	10.36	-6.5
	Beam FE–OpenSees [1]	15.89	-1.0	10.30	-5.5
	3–D FE Abaqus [2]	16.18	-0.5	–	–

Table 3. Maximum values of the bending moment for elastic soil M_{el} and inelastic soil M_{pl} in MPa and their location (m) from the ground level, for the Aegion (1995) excitation motion.

ACKNOWLEDGMENTS

The authors would like to acknowledge financial support from the EU 7th Framework research project funded through the European Research Council's Programme "Ideas", Support for Frontier Research – Advanced Grant, under Contract number ERC-2008-AdG 228254-DARE, and the Coordinator of the research project Professor George Gazetas.

REFERENCES

[1] S. Mazzoni, F. McKenna, G.L. Fenves, *OpenSees command language manual*, The Regents of the University of California, 2005.

[2] Dassault Systèmes Simulia Corp, *ABAQUS User's Manual, Providence*, RI, USA, 2009.

[3] S. Wang, B.L. Kutter, J.M. Chacko, D.W. Wilson, R.W. Boulanger, A. Abghari, Nonlinear seismic soil-pile-superstructure interaction, *Earthquake Spectra*, **14,** 377-396, 1998.

[4] E.J. Sapountzakis, A.E. Kampitsis, Nonlinear dynamic analysis of Timoshenko beam-columns partially supported on tensionless Winkler foundation, *Computers and Structures,* **88**, 1206–1219, 2010.

[5] E.J. Sapountzakis, V.G. Mokos, A BEM solution to transverse shear loading of beams, *Computational Mechanics*, **36**, 384-397, 2005.

[6] N. Makris, G. Gazetas, Dynamic pile-soil-pile interaction. Part II: Lateral and seismic response, *Earthquake Engineering and Structural Dynamics*, **21**, 145-162, 1992.

[7] H. Matlock, Correlations for design of laterally loaded piles in soft clay, *II Annual Offshore Technology Conference*, Houston, Texas, 1970.

[8] L.C. Reese, W.R. Cox, F.D. Koop, Field testing and analysis of laterally loaded piles in stiff clay, *VII Annual Offshore Technology Conference*, Houston, Texas, 1975.

[9] K.E. Brenan, S.L. Campbell, L.R. Petzold, N*umerical solution of initial-value problems in differential-algebraic equations*, North-Holland, Amsterdam, 1989.

[10] Z.P. Bazant, L. Cedolin, *Stability of structures: elastic, inelastic, fracture and damage theories*, Oxford University Press, New York, 1991.

[11] H.B. Seed, I.M. Idriss, *Soil moduli and damping factors for dynamic response analysis*, Report No. EERC 70-10, University of California, Berkeley, 1970.

[12] I.M. Idriss, J.I. Sun, SHAKE91: *A computer program for conducting equivalent linear seismic response analyses of horizontally layered soil deposits*, Center for Geotechnical Modeling Report, Department of Civil and Environmental Engineering, University of California, Davis, 1991.